



**University of  
Zurich**<sup>UZH</sup>

**Zurich Open Repository and  
Archive**

University of Zurich  
University Library  
Strickhofstrasse 39  
CH-8057 Zurich  
[www.zora.uzh.ch](http://www.zora.uzh.ch)

---

Year: 2010

---

## **Communication: Thermodynamics of water modeled using ab initio simulations**

Weber, V ; Asthagiri, D

**Abstract:** We regularize the potential distribution framework to calculate the excess free energy of liquid watersimulated with the BLYP-D density functional. Assuming classical statistical mechanical simulations at 350 K model the liquid at 298 K, the calculated free energy is found in fair agreement with experiments, but the excess internal energy and hence also the excess entropy are not. The utility of thermodynamic characterization in understanding the role of high temperatures to mimic nuclear quantum effects and in evaluating ab initio simulations is noted. 2010 American Institute of Physics. doi:10.1063/1.3499315

DOI: <https://doi.org/10.1063/1.3499315>

Posted at the Zurich Open Repository and Archive, University of Zurich

ZORA URL: <https://doi.org/10.5167/uzh-41034>

Journal Article

Published Version

Originally published at:

Weber, V; Asthagiri, D (2010). Communication: Thermodynamics of water modeled using ab initio simulations. *Journal of Chemical Physics*, 133(14):141101.

DOI: <https://doi.org/10.1063/1.3499315>

## Communication: Thermodynamics of water modeled using ab initio simulations

Valéry Weber and D. Asthagiri

Citation: *The Journal of Chemical Physics* **133**, 141101 (2010); doi: 10.1063/1.3499315

View online: <http://dx.doi.org/10.1063/1.3499315>

View Table of Contents: <http://scitation.aip.org/content/aip/journal/jcp/133/14?ver=pdfcov>

Published by the AIP Publishing

---

### Articles you may be interested in

Communication: Regularizing binding energy distributions and thermodynamics of hydration: Theory and application to water modeled with classical and ab initio simulations

*J. Chem. Phys.* **135**, 181101 (2011); 10.1063/1.3660205

Assessing the thermodynamic signatures of hydrophobic hydration for several common water models

*J. Chem. Phys.* **132**, 124504 (2010); 10.1063/1.3366718

Microscopic structure and thermodynamics of a core-softened model fluid: Insights from grand canonical Monte Carlo simulations and integral equations theory

*J. Chem. Phys.* **130**, 174504 (2009); 10.1063/1.3125930

Analysis of solvation structure and thermodynamics of methane in water by reference interaction site model theory using an all-atom model

*J. Chem. Phys.* **113**, 10240 (2000); 10.1063/1.1313788

Hydration free energy of hydrophobic solutes studied by a reference interaction site model with a repulsive bridge correction and a thermodynamic perturbation method

*J. Chem. Phys.* **113**, 2793 (2000); 10.1063/1.1305885

---

An advertisement for AIP Applied Physics Reviews. On the left is a thumbnail image of the journal cover, which features a 3D molecular model and a graph. The main text 'NEW Special Topic Sections' is in large white letters on a blue background with a bright light effect. Below this, on an orange background, it says 'NOW ONLINE' in yellow, followed by 'Lithium Niobate Properties and Applications: Reviews of Emerging Trends' in white. The AIP Applied Physics Reviews logo is in the bottom right corner.

**NEW Special Topic Sections**

**NOW ONLINE**  
Lithium Niobate Properties and Applications:  
Reviews of Emerging Trends

**AIP** Applied Physics  
Reviews

# Communication: Thermodynamics of water modeled using *ab initio* simulations

Valéry Weber<sup>1,a)</sup> and D. Asthagiri<sup>2,b)</sup>

<sup>1</sup>Physical Chemistry Institute, University of Zurich, 8057 Zurich, Switzerland

<sup>2</sup>Department of Chemical and Biomolecular Engineering, Johns Hopkins University, Baltimore, Maryland 21218, USA

(Received 9 August 2010; accepted 20 September 2010; published online 8 October 2010)

We regularize the potential distribution framework to calculate the excess free energy of liquid water simulated with the BLYP-D density functional. Assuming classical statistical mechanical simulations at 350 K model the liquid at 298 K, the calculated free energy is found in fair agreement with experiments, but the excess internal energy and hence also the excess entropy are not. The utility of thermodynamic characterization in understanding the role of high temperatures to mimic nuclear quantum effects and in evaluating *ab initio* simulations is noted. © 2010 American Institute of Physics. [doi:10.1063/1.3499315]

The liquid-vapor coexistence for water is thoroughly characterized experimentally, and the excess free energy (chemical potential) of a water molecule in the liquid relative to the vapor,  $\mu_w^{\text{ex}}$ , a basic descriptor of the liquid-vapor equilibrium, is very well-established.<sup>1</sup> The excess chemical potential, together with its derivatives, especially the temperature derivative (the excess entropy), is an essential quantity in understanding hydration phenomena and chemical transformations in the liquid state.

For *ab initio* simulations of water, two earlier studies<sup>2,3</sup> have sought  $\mu_w^{\text{ex}}$ . The first study revealed how the overbinding of water by PW91 (PBE) functionals leads to an overly negative chemical potential and ultimately an overstructured fluid. The second explored the coexisting densities of the liquid and vapor phases<sup>3</sup> and found a higher (lower) than normal vapor (liquid) density, suggesting overbinding of molecules by the BLYP functional. Their limitations notwithstanding, these early studies were incisive in evaluating the fluid simulated by *ab initio* dynamics.

In this communication, we present a rigorous calculation of the excess free energy using a theoretical approach that has matured over the past few years,<sup>4–6</sup> one that renders calculating free energies from *ab initio* simulations far less daunting than before. Together with an independent calculation of the excess internal energy, we obtain the excess entropy as well.

The relation between  $\mu_w^{\text{ex}}$  and intermolecular interactions is given by the potential distribution theorem<sup>7,8</sup>

$$\beta\mu_w^{\text{ex}} = \ln \int e^{\beta\varepsilon} P(\varepsilon) d\varepsilon, \quad (1)$$

where  $\varepsilon = U_N - U_{N-1} - U_w$  is the binding energy of the distinguished water molecule with the rest of the fluid.  $U_N$  is the potential energy of the  $N$ -particle system at a particular configuration,  $U_{N-1}$  is the potential energy of the configuration

but with the distinguished water removed, and  $U_w$  is the potential energy of the distinguished water molecule solely.  $P(\varepsilon)$  is the probability density distribution of  $\varepsilon$ .  $\mu_w^{\text{ex}}$  is the excess free energy in the liquid relative to an ideal gas at the same density and temperature. Based on the experimental coexistence densities<sup>1</sup> at 298 K,  $\mu_w^{\text{ex}} = -6.3$  kcal/mol.

A naive application of Eq. (1) to liquid water will fail because the high energy regions of  $P(\varepsilon)$ , reflecting the short-range repulsive interactions,<sup>5,9,10</sup> are never well sampled in a simulation. We resolve this difficulty by regularizing Eq. (1).<sup>10</sup> Consider a hard-core solute of radius  $\lambda$  centered on a distinguished water molecule: the hard-core solute excludes the remaining water oxygen atoms from within the sphere of radius  $\lambda$ . The chemical potential of the hard-core solute,  $\mu_{\text{HC}}^{\text{ex}}$ , is assumed known. With this construction, Eq. (1) can be rewritten as<sup>5,9,10</sup>

$$\beta\mu_w^{\text{ex}} = \beta\mu_{\text{HC}}^{\text{ex}} + \ln x_0 + \ln \int P(\varepsilon|n_\lambda=0) e^{\beta\varepsilon} d\varepsilon. \quad (2)$$

Here,  $P(\varepsilon|n_\lambda=0)$  is the binding energy distribution of the distinguished water molecule conditioned on there being no ( $n_\lambda=0$ ) water oxygen atoms within  $\lambda$  of the distinguished oxygen atom. By moving the boundary away from the distinguished water, we temper the interaction of the distinguished water with the rest of the fluid; indeed, for a sufficiently large  $\lambda$ ,  $P(\varepsilon|n_\lambda=0)$  is expected to be well-described by a Gaussian.<sup>5</sup> The fraction of configurations that do not have any oxygen atoms within  $\lambda$  of the distinguished oxygen is  $x_0$ ; this is the  $n=0$  member of the set  $\{x_n\}$  of coordination states sampled by the distinguished water molecule and characterizes the interactions between the distinguished water and the contents of the inner shell.<sup>4,7,11</sup> The excess chemical potential of the hard-core solute is  $\beta\mu_{\text{HC}}^{\text{ex}} = -\ln p_0$ , where  $p_0$  is the fraction of configurations in which a cavity of radius  $\lambda$  is found in the liquid.  $p_0$  is the  $n=0$  member of the set  $\{p_n\}$  of occupation numbers of a cavity and characterizes the packing interactions in hydration.<sup>12</sup>

<sup>a)</sup>Electronic mail: valeryweber@hotmail.com.

<sup>b)</sup>Electronic mail: dilipa@jhu.edu.

Since  $x_0$  and  $p_0$  are directly obtained from the simulation record, we only need explicit energy evaluations to compute the outer-shell contribution

$$\beta\mu_{\text{outer}}^{\text{ex}} = \ln \int P(\varepsilon|n_\lambda=0) e^{\beta\varepsilon} d\varepsilon. \quad (3)$$

Here, we calculate the outer-shell contribution using an alternative expression

$$\beta\mu_{\text{outer}}^{\text{ex}} = -\ln \int P^{(0)}(\varepsilon|n_\lambda=0) e^{-\beta\varepsilon} d\varepsilon, \quad (4)$$

where  $P^{(0)}(\varepsilon|n_\lambda=0)$  is the binding energy distribution in the uncoupled ensemble,<sup>4,7,10</sup> that is, after we find a suitable cavity in the liquid, we insert a test particle in that cavity and assess  $P^{(0)}(\varepsilon|n_\lambda=0)$ . The superscript (0) indicates that the test particle and the fluid are thermally uncoupled. It is advantageous to use Eq. (4) over Eq. (3) because the uncoupled distribution  $P^{(0)}(\varepsilon|n_\lambda=0)$  has a higher entropy than the coupled distribution  $P(\varepsilon|n_\lambda=0)$ , rendering the calculation of the free energy of inserting the particle [Eq. (4)] more robust than the free energy of extracting it [Eq. (3)].<sup>13</sup> Further, when  $x_0$  is small, it is difficult to characterize  $P(\varepsilon|n_\lambda=0)$  reliably, a limitation that does not apply to  $P^{(0)}(\varepsilon|n_\lambda=0)$ .

For  $\lambda$  sufficiently large such that  $P^{(0)}(\varepsilon|n_\lambda=0)$  is Gaussian distributed with a mean  $\langle\varepsilon|n_\lambda=0\rangle_0$  and variance  $\langle\delta\varepsilon^2|n_\lambda=0\rangle_0$  (the subscript 0 indicates that the test particle and the fluid are thermally uncoupled), Eq. (4) becomes

$$\mu_{\text{outer}}^{\text{ex}} = \langle\varepsilon|n_\lambda=0\rangle_0 - \frac{1}{2k_B T} \langle\delta\varepsilon^2|n_\lambda=0\rangle_0. \quad (5)$$

We apply the above framework to water simulated with the BLYP-D electron density functional. (In BLYP-D, the BLYP<sup>14,15</sup> functional is augmented with empirical corrections for dispersion interactions.<sup>16</sup>) We simulate the liquid at a density of 0.997 g/cm<sup>3</sup> (number density of 33.33 nm<sup>-3</sup>) and a temperature of 350 K. In this classical statistical mechanical simulation, the higher temperature effectively weakens the bonding<sup>6</sup> and has been found necessary to model the real liquid at the standard density and  $T=298$  K.<sup>6,17</sup> Note that while increasing the temperature mimics the effect of proton nuclear quantum effects for some properties,<sup>18–22</sup> the broad validity of this analogy is questionable.<sup>19,21,22</sup> Here, we study how well the thermodynamics of the classical fluid at 350 K approximates the thermodynamics of the real fluid at 298 K.

We simulate water with the CP2K code<sup>23</sup> and in the *NVE* and *NVT* ensembles; the electronic structure calculations are exactly as in our earlier study<sup>6</sup> and only salient differences are noted here. For the *NVT* ensemble simulations, we use the hybrid Monte Carlo method and extended the simulations in our earlier study of a 32 water system.<sup>6</sup> In the *NVE* ensemble, we simulated systems with 32 and 64 water molecules.

The production phase of the hybrid Monte Carlo lasted 2585 sweeps ( $\approx 130$  ps). The system temperature was 350 K. Simulations in the *NVE* ensemble lasted 200 ps of which the last 170 ps were used for analysis. The initial configuration for the 32 particle system was obtained from

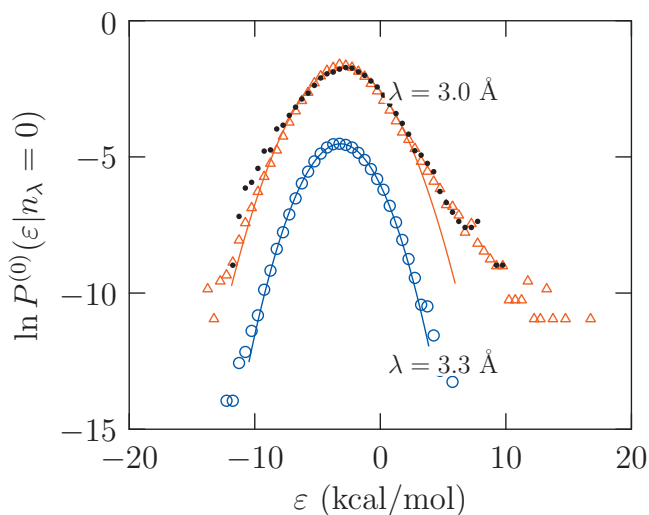


FIG. 1. Distribution of interaction energies  $P^{(0)}(\varepsilon|n_\lambda=0)$  for a distinguished water molecule at the center of an empty cavity of radius  $\lambda$ . The system comprises of 32 water molecules. The red triangles and blue circles are from the *NVE* simulation. The solid line defines the Gaussian model for the respective distribution. The black dots are from the *NVT* simulation. The  $\lambda=3.3$  Å curve has been shifted downward by 3 units for clarity. Observe that the thermodynamically important [Eq. (4)] low-energy tail is well-characterized. Further, for  $\lambda=3.3$  Å, both wings of the distribution are tempered and the Gaussian model becomes a good approximation.

the end-point of our earlier study.<sup>6</sup> The initial configuration for the 64 water system was obtained from an equilibrated configuration of SPC/E water<sup>24</sup> molecules. In the production phase, the average temperature was  $357 \pm 26$  K ( $362 \pm 19$  K) for the 32 (64) water system. The energy drift was less than 1.8 K (1.2 K) for the 32 (64) water system.

To calculate  $\mu_{\text{outer}}^{\text{ex}}$ , we construct a Cartesian grid within the simulation cell. The oxygen population within a radius  $\lambda$  of each grid center is calculated. In instances where there are no ( $n_\lambda=0$ ) water molecules, we insert a test water molecule in the cavity, assess its binding energy, and thus construct  $P^{(0)}(\varepsilon|n_\lambda=0)$ . (We draw water molecules from the simulation cell, randomly rotate it about an axis through the oxygen center, and use the resulting configuration as the test particle.)

In the *NVE* simulations, we first find approximately 3500 cavities from configurations sampled every 50 fs. (The target count of cavities is met by adjusting the spacing of the Cartesian grid between approximately 0.3 and 0.96 Å.) Thus, over 110k ( $\approx 32 \times 3500$ ) binding energy calculations are used to calculate  $\mu_{\text{outer}}^{\text{ex}}$  [Eq. (4)]. In the *NVT* simulations, the grid spacing for finding cavities to compute  $P^{(0)}(\varepsilon|n_\lambda=0)$  was fixed at 2.0 Å. For  $\lambda=3.0$  Å, this gave 98 cavities. In this instance, five different orientations were used for each test particle, giving about 16k ( $\approx 5 \times 32 \times 98$ ) binding energies to calculate  $\mu_{\text{outer}}^{\text{ex}}$ . Throughout, uncertainties in  $x_0$ ,  $p_0$ , and  $\langle e^{-\beta\varepsilon}|n_\lambda=0\rangle$  were estimated using the Friedberg and Cameron<sup>25</sup> block transformation procedure.<sup>26</sup>

Figure 1 shows  $P^{(0)}(\varepsilon|n_\lambda=0)$  for different cavity radii for the 32 water system. As the figure shows, the low energy region is well-characterized for inner-shell radii considered here; and it is this low- $\varepsilon$  part of the distribution that is most important for calculating  $\mu_{\text{outer}}^{\text{ex}}$  [Eq. (4)].

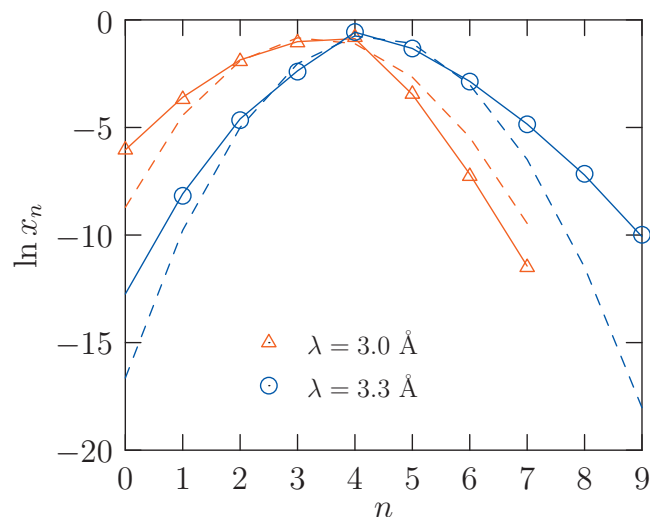


FIG. 2. Observed and estimated  $\{x_n\}$  for a  $N=64$  water molecule system and different inner-shell radii  $\lambda$ . Symbols denote the observed data. The solid line is obtained using Eq. (6). The dashed lines are maximum entropy fits using the mean and variance of  $\{x_n\}$  and a Gibbs prior (Ref. 27). Observe that  $\{x_n\}$  obtained using Eq. (6) well-describe the simulation results.

Figure 1 shows that the agreement between  $P^{(0)}(\epsilon|n_\lambda=0)$  obtained in the  $NVE$  and  $NVT$  simulations is satisfactory, although there is somewhat more scatter in the low-energy region for results with  $NVT$ . This is a consequence of using an order of magnitude less data (16k versus 110k) to construct  $P^{(0)}(\epsilon|n_\lambda=0)$ .

The probability  $x_0$  is a direct measure of the solute-water interactions within the inner shell, and perhaps not surprisingly, for large  $\lambda$ , this quantity is very low.<sup>11</sup> In this case, one can model  $\{x_n\}$  with a maximum entropy approach<sup>27</sup> using the robust estimates of mean and variance of  $\{x_n\}$ . However, for large  $\lambda$ ,<sup>4,6</sup> the underlying assumption of Gaussian occupancy statistics may not be valid. Here, we instead use Bayes's theorem in the form<sup>4</sup>

$$x_n = p_{n+1} \frac{p(1|n+1)}{\sum_{m \geq 1} p_m p(1|m)}, \quad (6)$$

where  $p(1|m)$  is the conditional probability of finding one

water molecule at the center of the cavity given that  $m$  water molecules are present in the cavity. For this purpose, following an earlier study,<sup>4</sup> the center is any point within 0.15 Å of the geometric center of the cavity.

Figure 2 depicts  $\{x_n\}$  for the 64 particle system. The fit using Eq. (6) is in excellent agreement with the actual data. This gives us confidence in the estimated  $x_0$  for  $\lambda=3.3$  Å (Fig. 2), an instance where  $x_0$  was not observed in the simulation. As Fig. 2 shows, the maximum entropy model can lead to errors in  $k_B T \ln x_0$  by about a kcal/mol or more, especially for the large  $\lambda$ .

Table I collects the various components of the excess chemical potential. Across the range of  $\lambda$ , the calculated values are within a kcal/mol (often less) of each other and the experimental value of  $-6.3$  kcal/mol for liquid water at 298 K. Comparing the 32 and 64 water results shows modest system size effect of about  $k_B T$ . This difference primarily arises from a less favorable  $\mu_{\text{outer}}^{\text{ex}}$  for the larger system: for a large cavity in a small simulation cell, the outer-shell water molecules pack tightly at the inner-shell water interface and lead to the lower  $\mu_{\text{outer}}^{\text{ex}}$ .

We can calculate the excess entropy of hydration per particle from the excess chemical potential and the mean binding energy  $\langle \epsilon \rangle$  of a distinguished water molecule in the fully coupled simulation. First, consider the excess internal energy. (Note that relative to the 64 particle case, in calculating  $\langle \epsilon \rangle$  for the 32 water system we used ten times as many values.) For the 32 (64) water system  $\langle \epsilon \rangle = -28.1 \pm 0.2$  kcal/mol ( $-27.3 \pm 0.8$  kcal/mol). Thus, the heat of vaporization per particle  $\Delta H_{\text{vap}} \approx -\langle \epsilon \rangle / 2 + k_B T = 14.8$  kcal/mol (14.4 kcal/mol) is substantially in error relative to the experimental value of about 10.5 kcal/mol at 300 K.<sup>1</sup> Neglecting small contributions due to the thermal expansion and compressibility of the medium, the excess entropy per particle<sup>5,10</sup> is  $S^{\text{ex}}/nk_B \approx \langle \epsilon \rangle / 2k_B T - \mu_w^{\text{ex}}/k_B T$ . Based on the estimates of  $\langle \epsilon \rangle$  and  $\mu_w^{\text{ex}}$ , it is seen that  $TS^{\text{ex}}$  for BLYP-D water is also in error.

In classical statistical mechanical simulations of liquid

TABLE I. Chemical ( $k_B T \ln x_0$ ), packing ( $k_B T \ln p_0$ ), and long-range interaction ( $\mu_{\text{outer}}^{\text{ex}}$ ) contributions to the excess chemical potential ( $\mu_w^{\text{ex}}$ ) of water obtained from  $NVE$  molecular dynamics simulations and  $NVT$  hybrid Monte Carlo simulations (Ref. 6). The radius of the inner shell is  $\lambda$  (in Å). The average temperatures of the  $N=32$  and  $N=64$  water systems are  $357 \pm 26$  K and  $362 \pm 19$  K, respectively. The temperature is 350 K for simulation in the  $NVT$  ensemble. Where available, the inner-shell chemical contribution is evaluated directly from the data, else the estimate using Eq. (6) is used. The outer-shell contribution is calculated using Eq. (4); estimates from a Gaussian model 5 (data in parenthesis) are provided for comparison. Energies are in kcal/mol. Uncertainties are at  $1\sigma$  level.

N	$\lambda$	$k_B T \ln x_0$		$-k_B T \ln p_0$	$\mu_{\text{outer}}^{\text{ex}}$	$\mu_w^{\text{ex}}$
		Simulation	Bayes			
32 (NVE)	3.0	$-4.3 \pm 0.1$	-4.3	$5.5 \pm 0.1$	$-7.1 \pm 0.2$ (-6.5)	$-5.9 \pm 0.2$
	3.1	$-5.6 \pm 0.1$	-5.5	$6.2 \pm 0.2$	$-6.5 \pm 0.2$ (-6.0)	$-5.9 \pm 0.3$
	3.2	$-7.2 \pm 0.4$	-6.8	$7.0 \pm 0.2$	$-6.2 \pm 0.2$ (-5.8)	$-6.4 \pm 0.5$
	3.3	$-8.5 \pm 0.6$	-8.6	$8.0 \pm 0.3$	$-5.7 \pm 0.1$ (-5.5)	$-6.2 \pm 0.7$
32 (NVT)	3.0	$-4.4 \pm 0.1$	-4.3	$5.2 \pm 0.3$	$-7.0 \pm 0.2$ (-7.2)	$-6.2 \pm 0.4$
64 (NVE)	3.0	$-4.4 \pm 0.0$	-4.3	$5.5 \pm 0.2$	$-6.8 \pm 0.5$ (-5.6)	$-5.7 \pm 0.5$
	3.1	$-5.8 \pm 0.1$	-5.7	$6.1 \pm 0.2$	$-5.8 \pm 0.3$ (-5.2)	$-5.5 \pm 0.4$
	3.2	$-7.2 \pm 0.2$	-7.2	$6.7 \pm 0.3$	$-5.3 \pm 0.1$ (-4.7)	$-5.8 \pm 0.4$
	3.3	Not observed	-9.2	$7.3 \pm 0.3$	$-4.8 \pm 0.1$ (-4.2)	-6.7



water with electron density functionals, both the limitations of the electronic structure model and the lack of nuclear quantum effects are intertwined. For example, simulations with BLYP at the same conditions as used here<sup>6</sup> gives  $\Delta H_{\text{vap}} = 12.0 \pm 0.5$  kcal/mol. Thus, excluding dispersion underbinds water molecules (see also Ref. 28) and leads to an apparently better agreement with experiments, but this agreement masks the limitations of BLYP in describing the phase behavior of water.<sup>3,6</sup> The intertwining noted above becomes apparent when we note that the difference in  $\Delta H_{\text{vap}}$  due to a change in the potential model is comparable to errors that can result from a classical description of the liquid.<sup>19,21,22</sup>

The present study shows that classical statistical mechanical simulations with BLYP-D at 350 K appears to adequately describe the structure<sup>6,17</sup> and the hydration free energy of the real liquid at 298 K. However, the agreement in free energy comes due to compensating deviations in the excess entropy and excess internal energy. This suggests that classical statistical mechanical simulations of water at 350 K with BLYP-D has limitations in describing the room temperature liquid; whether this reflects the limitations of the functional and/or of classical statistical mechanics remains unresolved. A resolution of this issue requires including nuclear quantum effects in BLYP-D based simulations, and such simulations, together with the theory presented here, could also prove decisive in elucidating the role of dispersion corrections in simulating water with electron density functional models.

The authors warmly thank Claude Daul (University of Fribourg) for computer resources. D.A. thanks the donors of the American Chemical Society Petroleum Research Fund for the financial support. This research used resources of the National Energy Research Scientific Computing Center, which is supported by the Office of Science of the U.S. Department of Energy under Contract No. DE-AC02-05CH11231.

- <sup>1</sup>W. Wagner and A. Pruss, *J. Phys. Chem. Ref. Data* **31**, 387 (2002).
- <sup>2</sup>D. Asthagiri, L. R. Pratt, and J. D. Kress, *Phys. Rev. E* **68**, 041505 (2003).
- <sup>3</sup>M. J. McGrath, J. I. Siepmann, I.-F. W. Kuo, C. J. Mundy, J. VandeVondele, M. Sprik, J. Hutter, F. Mohammed, M. Krack, and M. Parrinello, *J. Phys. Chem. A* **110**, 640 (2006).
- <sup>4</sup>A. Paliwal, D. Asthagiri, L. R. Pratt, H. S. Ashbaugh, and M. E. Paulaitis, *J. Chem. Phys.* **124**, 224502 (2006).
- <sup>5</sup>J. K. Shah, D. Asthagiri, L. R. Pratt, and M. E. Paulaitis, *J. Chem. Phys.* **127**, 144508 (2007).
- <sup>6</sup>V. Weber, S. Merchant, P. D. Dixit, and D. Asthagiri, *J. Chem. Phys.* **132**, 204509 (2010).
- <sup>7</sup>T. L. Beck, M. E. Paulaitis, and L. R. Pratt, *The Potential Distribution Theorem and Models of Molecular Solutions* (Cambridge University Press, Cambridge, 2006).
- <sup>8</sup>B. Widom, *J. Phys. Chem.* **86**, 869 (1982).
- <sup>9</sup>D. Asthagiri, H. S. Ashbaugh, A. Piryatinski, M. E. Paulaitis, and L. R. Pratt, *J. Am. Chem. Soc.* **129**, 10133 (2007).
- <sup>10</sup>D. Asthagiri, S. Merchant, and L. R. Pratt, *J. Chem. Phys.* **128**, 244512 (2008).
- <sup>11</sup>S. Merchant and D. Asthagiri, *J. Chem. Phys.* **130**, 195102 (2009).
- <sup>12</sup>L. R. Pratt, *Annu. Rev. Phys. Chem.* **53**, 409 (2002).
- <sup>13</sup>N. Lu and D. A. Kofke, *J. Chem. Phys.* **114**, 7303 (2001).
- <sup>14</sup>A. D. Becke, *Phys. Rev. A* **38**, 3098 (1988).
- <sup>15</sup>C. T. Lee, W. T. Yang, and R. G. Parr, *Phys. Rev. B* **37**, 785 (1988).
- <sup>16</sup>S. Grimme, *J. Comput. Chem.* **27**, 1787 (2006).
- <sup>17</sup>J. Schmidt, J. VandeVondele, I. F. W. Kuo, D. Sebastini, J. I. Siepmann, J. Hutter, and C. J. Mundy, *J. Phys. Chem. B* **113**, 11959 (2009).
- <sup>18</sup>R. A. Kuharski and P. J. Rossky, *J. Chem. Phys.* **82**, 5164 (1985).
- <sup>19</sup>B. Guillot and Y. Guissani, *J. Chem. Phys.* **108**, 10162 (1998).
- <sup>20</sup>E. Schwegler, J. C. Grossman, F. Gygi, and G. Galli, *J. Chem. Phys.* **121**, 5400 (2004).
- <sup>21</sup>L. Hernández de la Peña and P. G. Kusalik, *J. Am. Chem. Soc.* **127**, 5246 (2005).
- <sup>22</sup>F. Paesani, S. Iuchi, and G. A. Voth, *J. Chem. Phys.* **127**, 074506 (2007).
- <sup>23</sup>J. VandeVondele, M. Krack, F. Mohamed, M. Parrinello, T. Chassaing, and J. Hutter, *Comput. Phys. Commun.* **167**, 103 (2005).
- <sup>24</sup>H. J. C. Berendsen, J. R. Grigera, and T. P. Straatsma, *J. Phys. Chem.* **91**, 6269 (1987).
- <sup>25</sup>R. Friedberg and J. E. Cameron, *J. Chem. Phys.* **52**, 6049 (1970).
- <sup>26</sup>M. P. Allen and D. J. Tildesley, *Computer Simulation of Liquids* (Oxford University Press, Oxford, 1987), Chap. 6, pp. 192–195.
- <sup>27</sup>G. Hummer, S. Garde, A. E. Garcia, M. E. Paulaitis, and L. R. Pratt, *J. Phys. Chem. B* **102**, 10469 (1998).
- <sup>28</sup>G. Murdachaw, C. J. Mundy, and G. K. Schenter, *J. Chem. Phys.* **132**, 164102 (2010).